ADVANCED MATERIALS

Bio-inspired Bright Structurally Coloured Colloidal Amorphous Array Enhanced by Controlling Thickness and Black Background

Masanori Iwata[1], Midori Teshima[1], Takahiro Seki[1], Shinya Yoshioka[2]*, Yukikazu Takeoka[1]*

[1]*Department of Molecular Design & Engineering, Nagoya University, Furo-cho, Chikusa-ku, Nagoya 464-8603, Japan*
[2]*Department of Physics, Faculty of Science & Technology, Tokyo University of Science, 2641 Yamazaki, Noda 278-8510, Japan*

[*] Corresponding Author E-mail: ytakeoka@apchem.nagoya-u.ac.jp, syoshi@rs.tus.ac.jp

[**] Y. T. acknowledges the support of Grants-in-Aid for Scientific Research (No. 15H02200 and No. 22107012) in Innovative Areas: “Fusion Materials” (Area No. 2206) from the Ministry of Education, Culture, Sports, and Science (MEXT). S. Y. acknowledges the support of a Grant-in-Aid for Scientific Research (No. 24120004) in Innovative Areas: “Innovative Materials Engineering Based on Biological Diversity” (Area No. 4402) from MEXT.

Abstract

Inspired by Steller's jay that displays angle-independent structural colours, we created angle-independent structurally coloured materials that are composed of amorphous arrays of submicron-sized fine spherical silica colloidal particles. When the colloidal amorphous arrays are thick, they do not appear colourful but almost white. However, the saturation of the structural colour can be increased by (i) appropriately controlling the thickness of the array and (ii) placing the black background substrate. These situations are similar in the case of the blue feather of Steller's jay. Based on the knowledge gained through the bio-mimicry structural coloured materials, colloidal amorphous arrays on the surface of a black particle as the core particle were also prepared as colourful photonic pigments. Moreover, we successfully built a structural colour on-off system by controlling the background brightness of the colloidal amorphous arrays.

Keywords: angle-independent structural colour, black background, photonic pigment, colloidal amorphous array, bio-inspired

Structural colour is often explained as follows: “Structural colour is brilliant iridescent colour caused by the interaction between a visible light and periodical refractive index structured materials, which are comparable to the wavelength of visible light.” However, this explanation is not entirely correct. Recently, a number of studies confirmed that materials found in both living[1, 2] and artificial[3, 4-8] objects with only a short-range order can display structural colours. It is interesting that such structural colours are virtually independent of the angle of observation. However, these materials do not always appear colourful; the wavelength-independent multiple scattering often makes them appear white. Recent studies have reported that these potential nanostructured materials require black substances to enhance the structural colours[4, 5, 7]. In fact, it is known that many natural examples of structural colours are enhanced by the presence of dark materials. For example, the brilliant blue feathers of some bird species have amorphous spongy network structures that cause structural colours, which are enhanced by underlying black melanin particles[2].

Inspired by well-designed biological structurally coloured materials, we and other groups have attempted to mimic these materials by using the amorphous aggregation of fine colloidal particles. The amorphous system appears almost white, when it is thick because of the incoherent multiple scattering. This is in contrast to the system having a long-range order like a photonic crystal; the perfect photonic crystals do not scatter light and, thus, they do not appear white even when the system is thick. Thus, researchers have developed a way to enhance the structural colour of the amorphous system; the addition of small black substances, such as carbon black, magnetite, and metal micro-particles, into aggregations of fine colloidal particles, has been found effective to make these aggregations appear recognizable beautiful structural colours [4-6, 9]. However, the amorphous system with small black additives is different from the above-mentioned biological structural colours, because for example in the blue bird feathers the black melanin particles are located below the colour-causing structures. How does this difference affect the appearance of the material? Placing the black materials under the amorphous aggregation should be effective to reduce the influences of reflection from the substrate and further underlying materials, while the aggregation may appear white when it is very thick, implying that there is an optimal thickness for the colouration. On the other hand, dispersing black materials throughout the aggregation should decrease the total amount of reflection, because the light that dwells inside it is absorbed. If we can accurately reproduce biological structural coloured materials with a separated structure between the colour-causing structures and black substances, we may be able to acquire the necessary information to develop a more efficient design of structurally coloured functional materials. Here, we first describe the preparation and optical properties of bio-inspired angle-independent structurally coloured materials composed of colloidal amorphous arrays of submicron-sized fine sphere colloidal particles that are fabricated on the surface of a black plate.

It is important to control the thickness of the colloidal amorphous arrays to investigate the effects of the underlying black materials on the structural colouration. In this study, we employed the Layer-by-Layer method (LbL method)[10], in which a large area of uniform membranes is prepared by depositing alternating layers of oppositely charged materials with wash steps between each layer, to form the colloidal amorphous arrays of charged submicron-sized fine colloidal particles and an oppositely charged polyelectrolyte (Fig. 1a). A negatively charged silica colloidal particle was used as the

charged colloidal particles, and a black quartz plate impregnated with carbon black was used as the black background. A transparent glass plate was also used for comparison. As glue between the silica particles layers, poly(diallyldimethylammonium chloride) (PDDA) was employed, which can be positively charged in water. The surfaces of both the commercial black quartz plate and the transparent glass plate were cleaned using KOH-saturated ethanol, which induced a negative charge. Thus, at the beginning, these plates were immersed into the PDDA aqueous solution to achieve positively charged surfaces for preparing the first colloidal amorphous array layer. The excess PDDA was thoroughly washed away by soaking the plates in a sufficient amount of water three times. After this step, these positively charged plates were immersed into the silica particle aqueous suspension to prepare the silica particle-adsorbed plates, which was followed by three washing steps to remove the unbound silica particles. We prepared membrane-like colloidal amorphous arrays composed of fine silica particles and PDDA on each plate by repeating the above-described series of operations, which are defined as one cycle.

Fig. 1b and 1c show the scanning electron microscope (SEM) images of the surface of the membranous colloidal amorphous arrays prepared by 5 cycles of the LbL method and the interior of the membranes prepared by different numbers of cycles, respectively. A silica colloidal particle of 190 nm in diameter was used to obtain these membranes. The surface SEM image was analysed using the Fourier transform (FT) and resulted in a ring-patterned power spectrum, which is shown in the inset in Fig. 1b. This pattern indicates that the silica particles form an isotropic colloidal amorphous array with only a short-range order[11]. We found that homogeneous colloidal amorphous arrays were obtained using this LbL method irrespective of the number of layers of the membranes because similar ring-patterned FT images were observed for each membrane (Supporting Information Fig. S3). We confirmed that the thickness of the colloidal amorphous arrays estimated from the cross-sectional SEM image in Fig. 1c linearly increases with the cycles of the LbL procedure. The increase in the thickness of the membrane per each LbL procedure was found to be 140 nm from a linear fitting analysis shown in Fig. 1d, which is smaller than the diameter of the silica particle.

Fig. 2a shows a photograph of the colloidal amorphous arrays composed of silica colloidal particles 190 nm in diameter and PDDA with different thicknesses prepared on a transparent glass plate and black quartz plate. In the case of the colloidal amorphous arrays on the black quartz plate, more vibrant blue colour were observed as the thickness of the array increased up to 15 cycle. On the other hand, the colloidal amorphous arrays on the transparent glass plate all show more white tinges than those on the black quartz plate. Figure 2b shows the reflectance spectra for 15 cycles. It is common for both the substrates that reflectance peak is located around 400 nm. However, the reflectance of the transparent substrate is higher than the black one over the entire wavelength range examined. The spectrum looks like a sum of a constant background and the spectrum of the black substrate. When the substrate is transparent, the light can be reflected back from the bottom surface of the substrate, and furthermore, the light can be scattered back from things under the substrate. These reflections could affect the appearance of the colloidal amorphous arrays. By contrast, such background scattering can be removed when the black quartz is used as the substrate because the transmittance of visible light through the black quartz is less than 1 % at 500 nm.

To clearly demonstrate the effects of the background scattering, we tried to reduce it

for the sample on the transparent glass plate by a refractive index matching method[8]. Fig. 2c shows photographs of (i) the colloidal amorphous array composed of silica colloidal particles 190 nm in diameter and PDDA on a transparent glass plate placed on a black plastic board with a rough surface and (ii) the same sample shown in (i), except the interstices between the transparent glass plate and black plastic board were filled with water. The reflection from the bottom surface of the substrate and the scattering from the rough surface of the black board are thought to be almost wavelength-independent. Thus, the appearance of the colloidal amorphous array shown in (i) becomes whitish. However, the impregnation of water decreased such wavelength-independent reflection because the refractive index of water is more close to those of the substrate and the black plastic board than air. As a result, the saturation of the colours of the colloidal amorphous array is increased in (ii).

Figure 2a shows that the thickness of the amorphous colloidal array is another key factor to produce a saturate structural colour; when the amorphous colloidal array is too thick, the colour becomes whitish. In fact, as shown in Fig. 2d, reflectance spectrum of the colloidal amorphous array even on the black quartz gradually increased as the cycle of LbL process was increased in the entire wavelength of the visible light. In the spectrum of 50 cycles, reflectance at a wavelength longer than 600 nm is not negligible, and that is consistent with the appearance of white colour. On the other hand, the wavelength of the reflectance peak does not depend on the thickness, indicating that hue is solely determined by the characteristic length of the short-range order of amorphous colloidal array. Thus, the thickness of the array should be controlled to obtain saturated structural colour of the colloidal amorphous arrays.

It is likely that the multiple incoherent scattering within the colloidal amorphous array is one origin that lowers the saturation of the colour[4, 12], in particular when the system is thick. To examine this hypothesis, we measured the polarization dependent reflection spectra of the colloidal amorphous array on the black quartz plate. The spectra were obtained using the methods shown in Figs. S5b and S5c. White light was passed through a linear polarizer and then illuminated onto the colloidal amorphous array. The incident angle relative to the normal to the planar surface of the colloidal amorphous array was 0°. The polarization of the incident light was parallel to the scattering plane containing the incident beam and detector. The detector was placed at a fixed angle of 10° to the surface normal. Another linear polarizer was placed in front of the detector, and the polarization direction was changed to be parallel (co-polarization) or perpendicular (cross-polarization) to the scattering plane. Fig. 2e shows the polarization spectra obtained for the colloidal amorphous array on the black quartz plate composed of 190 nm silica particles and PDDA using 10 and 50 cycles of the LbL method. In the spectrum of the co-polarized light scattered from the colloidal amorphous array for the sample with 10 cycles, a distinct spectral peak was observed at approximately 400 nm, whereas the cross-polarized reflectance spectrum was much lower than the co-polarized one, and spectral peaks were not observed in the entire range of the investigated wavelengths. The fact that the reflectance peak was only observed in the co-polarization spectra implies that the peak was produced by the optical interference of single scatterings from individual particles because single scattering processes do not depolarize light[13]. When the thickness of the sample is increased to the case of, for example, the sample with 50 LbL cycles, co-polarized reflectance increased, but the spectral purity decreased as shown in Fig. 2e; not only the reflectance at the peak at

approximately 400 nm, but the overall reflectance also increased in the entire wavelength range. Correspondingly, reflectance in the cross-polarization spectrum also increased. This indicates that the multiple and incoherent light scattering, which could depolarize the reflection, occur inside the colloidal amorphous array.

To estimate the most favourable thickness for the colloidal amorphous arrays on the black quartz plate that display brilliant structural colour, we investigated the effect of the thickness on the colour saturation, which includes the effect of lightness, using the chromaticity coordinate obtained from the relative reflectance measurement (Supporting Information Fig. S8). The dominant wavelength, which is defined as the peak wavelength observed at approximately 375 nm in the relative reflectance spectra, does not depend on the thickness, which indicates that thickness has an insignificant effect on the hue. The lightness, L^*, increases as the thickness increases (Supporting Information Fig. S8c). $C^*_{u,v}$, which expresses the amount of shade, is independent of the lightness, although it also increases as the thickness increases (Supporting Information Fig. S8d). A type of saturation, $S_{u,v}$, which is correlated with the lightness, and estimated by using L^* and $C^*_{u,v}$, increases as the thickness increases up to 1.75 μm, although it decreases as the thickness increases above this threshold (Fig. 2f). This trend is prominently expressed for the colloidal amorphous arrays on the black quartz plate. Judging from the results above, the optimum thickness of the colloidal amorphous arrays on the black quartz plate that displays the most saturated structural colours is between approximately 1 and 2 μm. It is interesting that this value is comparable to the thickness of the air-keratin spongy layer (2～3 μm) found in the non-iridescent blue structural coloured plumage of a Steller's jay, in which a black basal melanin layer underlies the spongy layer[2]. As demonstrated above, enhancing the saturation of the colour of the colloidal amorphous array requires the (i) absorption of transmitting light by the black background substrate and (ii) adequate control of the thickness of the colloidal amorphous array.

It is desirable for the structurally coloured material to show the same colour independently on the angle of observation, if it is used for general-purpose pigments. Fig. 2g shows the angle-dependent scattering spectra of the colloidal amorphous arrays on the black quartz plate with 50 cycles of the LbL method. The scattering spectra were measured by changing only the detection angle, whereas the incidence angle remained fixed. The incidence angle relative to the normal angle of the surface of the array was 0°. The detection angle θ was varied from 10° to 60°. The wavelength of the spectral peak was found to be remained approximately the same. This feature confirms that the colour of the prepared material does not change with the angle of observation.

The colloidal amorphous arrays displaying different hues can be easily prepared using different-sized silica particles. When using 260 and 300 nm diameter silica particles, we can obtain colloidal amorphous arrays that display a vivid green and purplish red colour, respectively (Fig. 2h). The colour is directly related to the size of the silica particle as is explained in previous studies [1,13]. The optimum thickness for the green and purplish red colours that exhibits the most saturated colours is also found to be approximately 1 ～2 μm.

In our previous research[4], it was found that the amorphous aggregation with small black additives exhibits angle-independent saturated structural colour even when the system is thick. On the other hand, the present system needs to be thin and also requires a black substrate in order to appear colourful. For a case that the amorphous system is

thin, major part of the incident light can reach the background and reflected light from the substrate can lower the saturation of the structural colour. As the thickness of the colloidal amorphous arrays increases, the reflection and the scattering from the back are reduced, but the contribution of the incoherent scattering from the inside of the arrays becomes larger. As a result, it is difficult to observe vivid colors from the colloidal amorphous arrays formed on a transparent glass plate. If the background of the colloidal amorphous arrays is black, when the thickness of the colloidal amorphous arrays is small, there is no reflection or scattering from the back, so a vivid structural color due to the coherent scattering can be observed. Although the fabrication of the black-additive approach seems simpler, the present system is potentially environmentally friendly because the materials used for the coloration can be minimized; only 1～2 μm- thick amorphous array is necessary. Moreover, the present system can be developed into several applications described below.

The combination of colloidal amorphous arrays and a black background is applicable for the preparation of dispersible colourful pigments. A fine polystyrene particle of 5 μm that includes carbon black was used as the core material to prepare such pigments. Because this polystyrene particle has a negative charge at the surface, the LbL method can be used to prepare colloidal amorphous arrays on the polystyrene particles using fine silica particles and PDDA (Supporting Information, Fig. S18), which resulted in raspberry-shaped particles (Fig. 3a, b). Similar to the colloidal amorphous arrays on the flat black quartz plate, the saturation of the colours observed for the raspberry-shaped particles increases as the thickness of the colloidal amorphous arrays on the core particles increases (Fig. 3c, d). These angle-independent raspberry-shaped structural coloured particles may be useful as dispersible pigments. As shown in Figure 3c, the saturation of the colour is increased as the increase in the thickness of the colloidal amorphous array portion. As one can expect, however, the colloidal amorphous array portion also includes the effect of the inter-particle multiple scattering. Thus, the colour saturation is expected to be improved when the thickness of the colloidal amorphous array is optimized.

As shown in Fig. 2a and 2c, the saturation of the structural colours from the colloidal amorphous arrays largely depends on the blackness of the background (Supporting Information Fig. S17). If the blackness behind the colloidal amorphous arrays can be controlled, the colour saturation can be manipulated, even if the arrays are prepared on a transparent substrate. We demonstrated it by using a simple experimental setup shown in Fig. 4a. Configuring the primary and secondary polarizing plates in the orthogonal direction of each transmitting linearly polarized ray will cut the light. This state is called crossed nicols and appears dark background. However, under parallel nicols, in which the primary polarizing plate is rotated so that the direction of the transmitted linearly polarized light matches the secondary polarizing plate, backscattered light becomes strong. Thus, we can control the blackness just by changing the direction of the two-stacked polarizing plates. Fig. 4b shows the colloidal amorphous arrays composed of different-sized fine silica particles and PDDA prepared on a transparent glass plate, which are placed on the two-stacked polarizing plates. The colours appeared whitish when the two-stacked polarizing plates become parallel nicols, whereas the structural colours are more vibrant when the background is dark by changing the directions of these polarizing plates (Fig. 4b, and Supporting Information Movie 1).

During the course of evolution, it is presumably thought that animals have optimized

their important functions, such as body colouration that is used for the conspecific communication. As mentioned above, it is interesting that optimized thickness of colloidal amorphous array is comparable with the spongy layer overlying the black basal melanin layer in the non-iridescent blue structural coloured plumage of a Steller's jay. If we can unravel the mechanisms underlying these biological optical phenomena, we can mimic the biological systems using artificial materials by accounting for important factors.

Acknowledgements
This work was supported by Grants-in-Aid for Scientific Research (No. 23245047, No. 22340121, No. 22107012, and No. 24120004) in the Innovative Areas of “Fusion Materials” (Area No. 2206) and "Innovative Materials Engineering Based on Biological Diversity" (Area No. 4402) from the Ministry of Education, Culture, Sports, Science and Technology (MEXT). A fine black polystyrene particle is kindly provided from Sekisui Chemical Co. Ltd.

Author contributions
Y. T. designed the project. M. I. and M. T. performed the experiments. All authors discussed the results and contributed to interpreting the data. Y. T. and S. Y. wrote the manuscript. Y. T. and S. Y. commented on the manuscript.

Additional information
Supplementary Information accompanies this paper at http://www.

References

[1] H. Noh, S. F. Liew, V. Saranathan, S. G. J. Mochrie, R. O. Prum, E. R. Dufresne, H. Cao, Adv Mater 2010, 22, 2871; R. O. Prum, R. H. Torres, J Exp Biol 2004, 207, 2157; L. Shi, Y. F. Zhang, B. Q. Dong, T. R. Zhan, X. H. Liu, J. Zi, Adv Mater 2013, 25, 5314.

[2] M. D. Shawkey, G. E. Hill, J Exp Biol 2006, 209, 1245.

[3] Y. Takeoka, M. Honda, T. Seki, M. Ishii, H. Nakamura, Acs Appl Mater Inter 2009, 1, 982; M. Harun-Ur-Rashid, A. Bin Imran, T. Seki, M. Ishi, H. Nakamura, Y. Takeoka, Chemphyschem 2010, 11, 579; Y. Gotoh, H. Suzuki, N. Kumano, T. Seki, K. Katagiri, Y. Takeoka, New J Chem 2012, 36, 2171; R. Hirashima, T. Seki, K. Katagiri, Y. Akuzawa, T. Torimotoa, Y. Takeoka, J Mater Chem C 2014, 2, 344; Y. Ohtsuka, T. Seki, Y. Takeoka, Angew Chem Int Edit 2015, 54, 15368; M. Kohri, Y. Nannichi, T. Taniguchi, K. Kishikawa, J Mater Chem C 2015, 3, 720; J. G. Park, S. H. Kim, S. Magkiriadou, T. M. Choi, Y. S. Kim, V. N. Manoharan, Angew Chem Int Edit 2014, 53, 2899; K. Ueno, Y. Sano, A. Inaba, M. Kondoh, M. Watanabe, J Phys Chem B 2010, 114, 13095; F. Wang, X. Zhang, Y. Lin, L. Wang, J. F. Zhu, Acs Appl Mater Inter 2016, 8, 5009; M. Xiao, Y. W. Li, M. C. Allen, D. D. Deheyn, X. J. Yue, J. Z. Zhao, N. C. Gianneschi, M. D. Shawkey, A. Dhinojwala, Acs Nano 2015, 9, 5454; C. F. Lai, Y. C. Wang, H. C. Hsu, J Mater Chem C 2016, 4, 398.

[4] Y. Takeoka, S. Yoshioka, A. Takano, S. Arai, K. Nueangnoraj, H. Nishihara, M. Teshima, Y. Ohtsuka, T. Seki, Angew Chem Int Edit 2013, 52, 7261.

[5] Y. Takeoka, S. Yoshioka, M. Teshima, A. Takano, M. Harun-Ur-Rashid, T. Seki, Sci Rep-Uk 2013, 3.

[6] M. Teshima, T. Seki, R. Kawano, S. Takeuchi, S. Yoshioka, Y. Takeoka, J Mater Chem C 2015, 3, 769.

[7] J. D. Forster, H. Noh, S. F. Liew, V. Saranathan, C. F. Schreck, L. Yang, J. G. Park, R. O. Prum, S. G. J. Mochrie, C. S. O'Hern, H. Cao, E. R. Dufresne, Adv Mater 2010, 22, 2939.

[8] D. T. Ge, L. L. Yang, G. X. Wu, S. Yang, J Mater Chem C 2014, 2,

4395.
[9] Y. Takeoka, J Mater Chem 2012, 22, 23299; Y. Takeoka, J Mater Chem C 2013, 1, 6059.
[10] G. Decher, J. D. Hong, Makromol Chem-M Symp 1991, 46, 321; R. K. Iler, J Colloid Interf Sci 1966, 21, 569; K. Ariga, J. P. Hill, Q. M. Ji, Phys Chem Chem Phys 2007, 9, 2319; K. Katagiri, S. Yamazaki, K. Inumaru, K. Koumoto, Polym J 2015, 47, 190; K. W. Tan, G. Li, Y. K. Koh, Q. F. Yan, C. C. Wong, Langmuir 2008, 24, 9273; J. J. Richardson, M. Bjornmalm, F. Caruso, Science 2015, 348.
[11] R. O. Prum, R. H. Torres, S. Williamson, J. Dyck, Nature 1998, 396, 28.
[12] S. Yoshioka, Y. Takeoka, Chemphyschem 2014, 15, 2209.
[13] H. Noh, S. F. Liew, V. Saranathan, R. O. Prum, S. G. J. Mochrie, E. R. Dufresne, H. Cao, Optics Express 2010, 18, 11942.

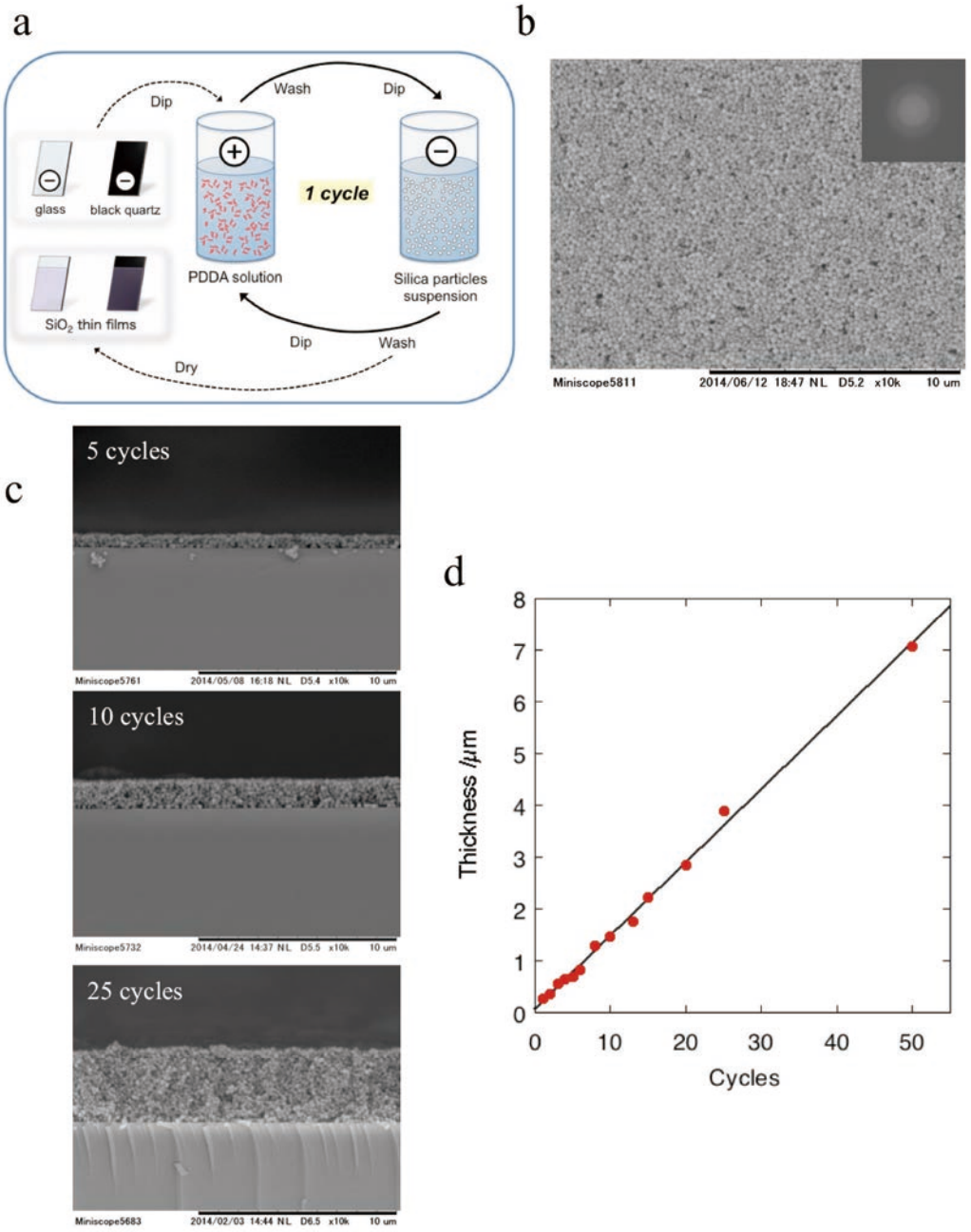

Figure 1 a: Preparation method to construct a colloidal amorphous array composed of silica particles and PDDA on a clear glass plate or a black quartz plate using the LbL method. b: Surface SEM image of the colloidal amorphous array composed of 190 nm silica colloidal particles and PDDA prepared using 5 cycles of the LbL method. c: Cross-sectional SEM images of the colloidal amorphous arrays with different thicknesses. d: Plots showing the thickness of the colloidal amorphous arrays *versus* the number of cycles of the LbL method.

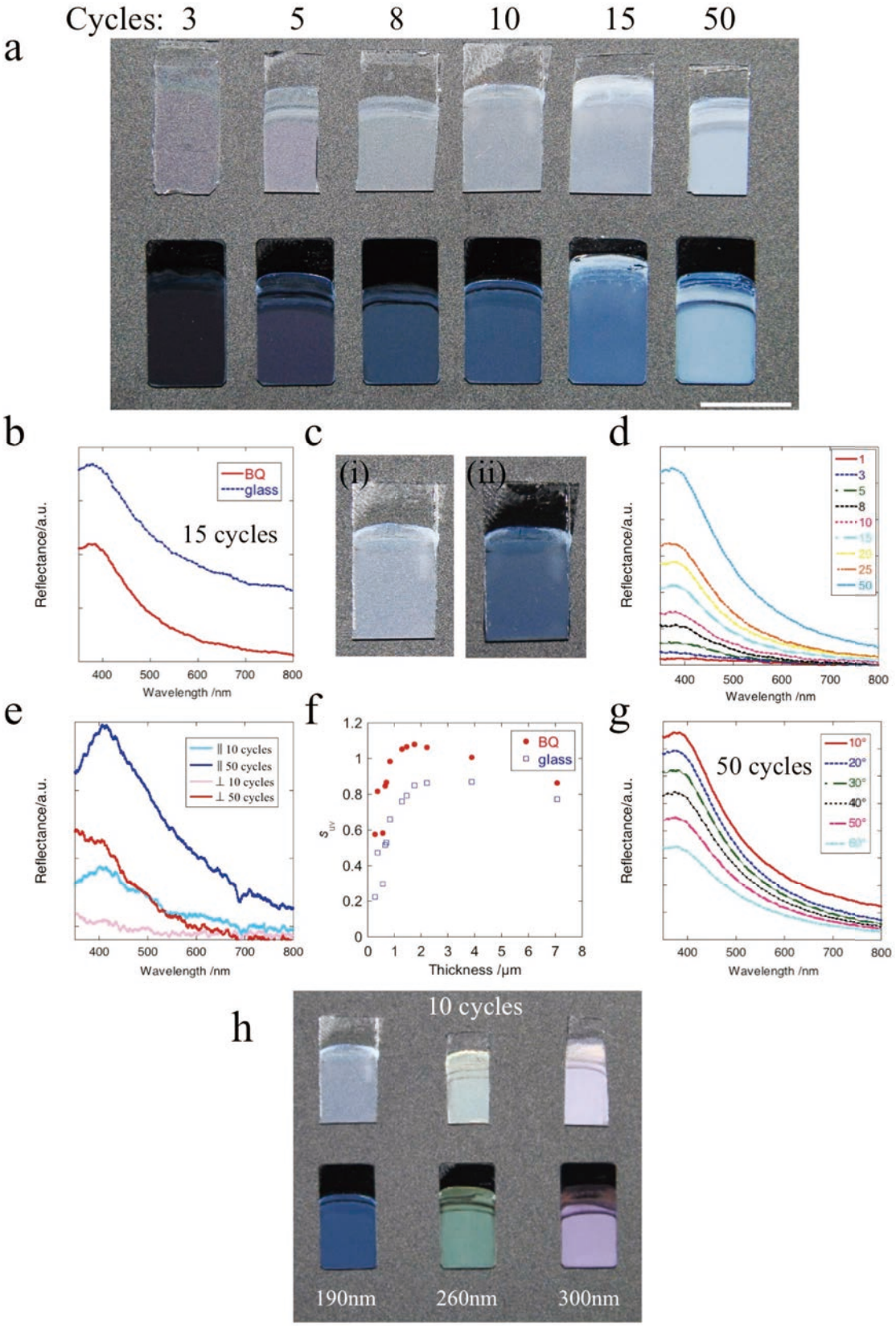
Cycles: 3 5 8 10 15 50
a
b
BQ
glass
15 cycles
Reflectance/a.u.
Wavelength /nm
c
(i)
(ii)
d
1
3
5
8
10
15
20
25
50
Reflectance/a.u.
Wavelength /nm
e
∥ 10 cycles
∥ 50 cycles
⊥ 10 cycles
⊥ 50 cycles
Reflectance/a.u.
Wavelength /nm
f
BQ
glass
s_{uv}
Thickness /μm
g
50 cycles
10°
20°
30°
40°
50°
60°
Reflectance/a.u.
Wavelength /nm
h
10 cycles
190nm
260nm
300nm

Figure 2 a: Optical picture of the colloidal amorphous arrays with different thicknesses composed of 190 nm silica particles and PDDA prepared on a clear glass plate and black quartz plate. b: Scattering spectra of the colloidal amorphous arrays composed of 190 nm silica particles and PDDA prepared on a clear glass plate and black quartz plate (BQ). The number of cycles of LbL is 15. c: Photographs of (i) the colloidal amorphous array composed of silica colloidal particles 190 nm in diameter and PDDA on a clear glass plate using 10 cycles of the LbL method and placed on a black plastic board with a rough surface; (ii) is the same sample shown in (i) placed on a black plastic board with a rough surface, except the interstices between the clear glass plate and the black plastic board were filled with water. d: Scattering spectra of the colloidal amorphous arrays of different thicknesses composed of 190 nm silica particles and PDDA prepared on the black quartz plate. e: Polarization spectra (∥ : co-polarized spectra, ⊥ : cross-polarized spectra) obtained for the colloidal amorphous array composed of 190 nm silica particles and PDDA on a black quartz plate using 10 cycles and 50 cycles of the LbL method. f: Plots showing the value of S_{UV} as a function of the thickness of the colloidal amorphous arrays composed of 190 nm silica particles and PDDA prepared on a clear glass plate and black quartz plate (BQ). g: Angle-dependent scattering spectra of the colloidal amorphous arrays on a black quartz plate with 50 cycles of the LbL method; the spectra are measured by changing the detection angle, with the incidence angle remaining fixed. The incidence angle relative to the normal angle of the surface of the array was 0°. The detection angle θ was varied from 10° to 60°. h: Optical picture of the colloidal amorphous arrays with different-sized silica particles of 190, 260, and 300 nm with PDDA prepared on a clear glass plate and black quartz plate. The number of cycles of LbL is 10.

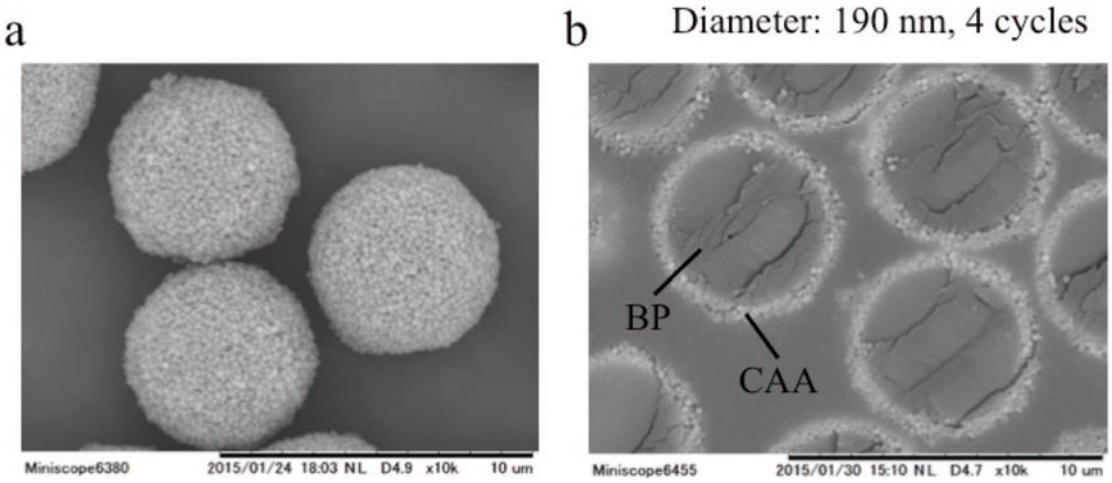
a
b
Diameter: 190 nm, 4 cycles
BP
CAA
Miniscope6380
2015/01/24 18:03 NL D4.9 x10k 10 um
Miniscope6455
2015/01/30 15:10 NL D4.7 x10k 10 um

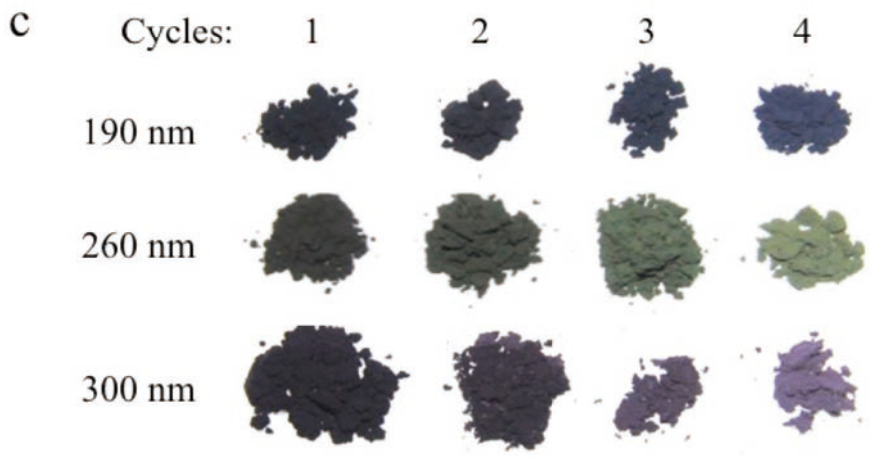
c
Cycles: 1 2 3 4
190 nm
260 nm
300 nm

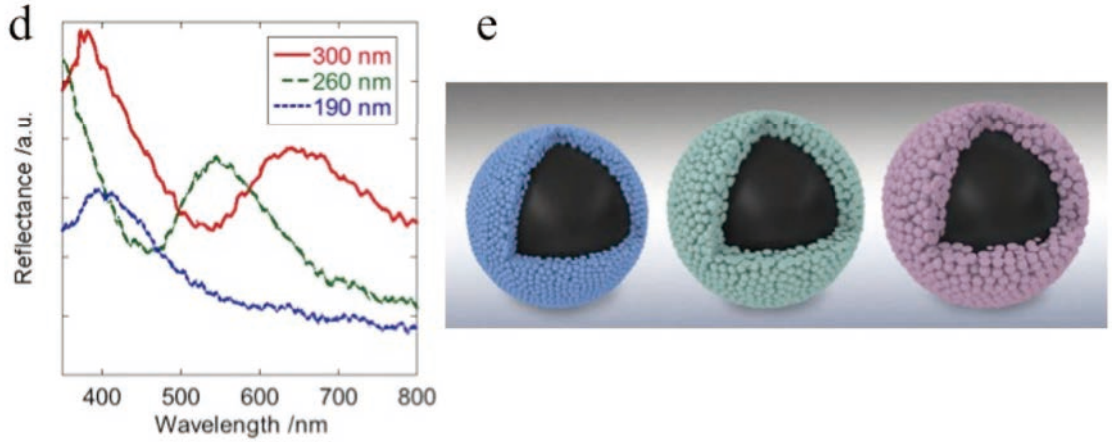
d
e
300 nm
260 nm
190 nm
Reflectance /a.u.
400 500 600 700 800
Wavelength /nm

Figure 3

Figure 3 a: SEM image of the raspberry-shaped particles prepared using a negatively charged fine black polystyrene particle to form a 5 μm core with 190 nm silica particles and PDDA to form a colloidal amorphous array as the shell. The number of cycles of LbL is 4. b: Cross-sectional SEM image of the raspberry-shaped particles shown in Fig. 3a. BP stands for black polystyrene particle and CAA for colloidal amorphous array. c: Photograph showing the changes in saturation and hue of the raspberry-shaped particles, which are dependent on the number of layers and size of the silica particles, respectively. d: Scattering spectra of the raspberry-shaped particle using different-sized particles with 4 cycles of the LbL method. e: Schematic representation of the structurally coloured raspberry-shaped particle.

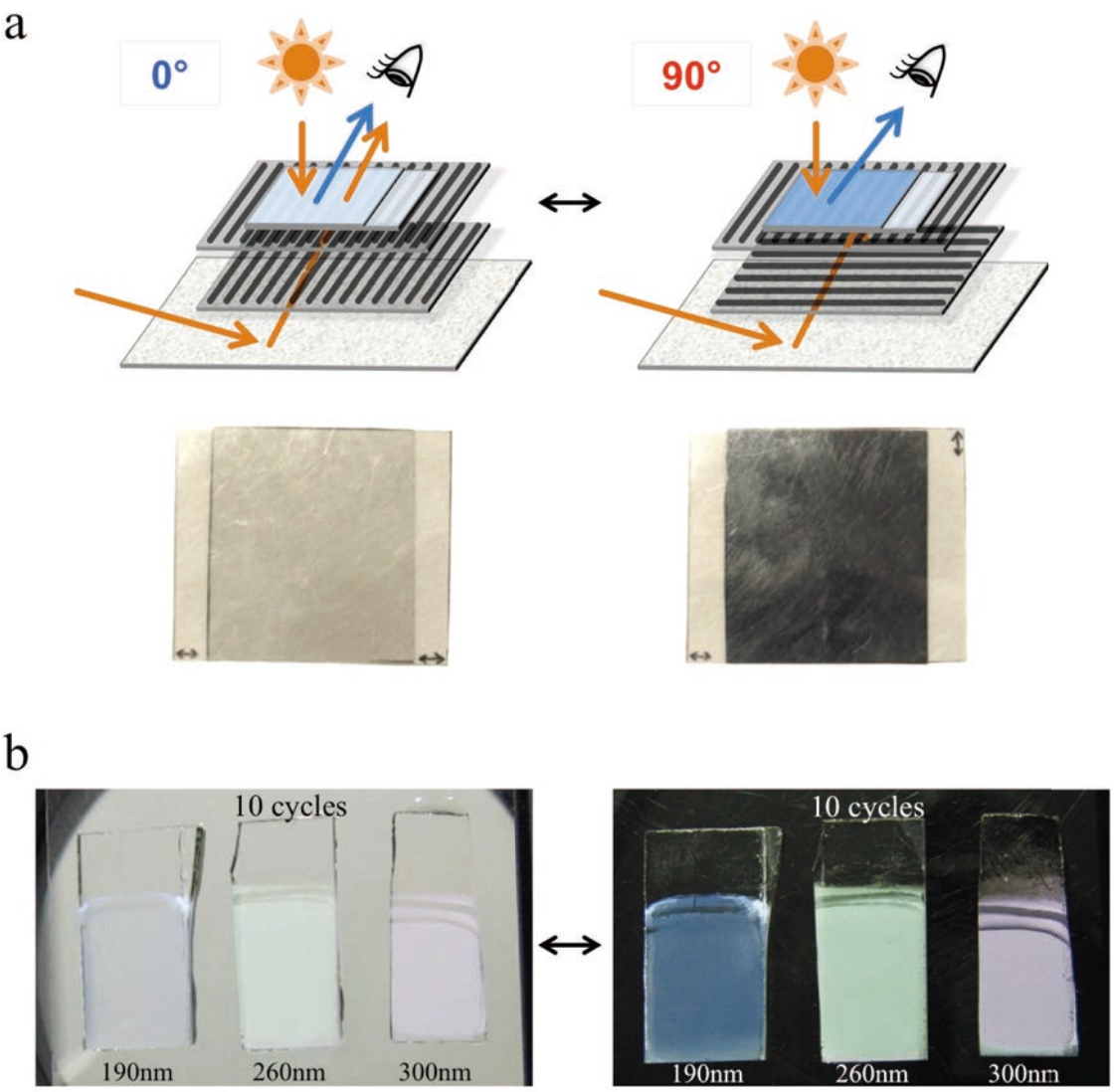

Figure 4 a: Conceptual images and optical photographs of the parallel nicols and crossed nicols. b: Optical images of the colloidal amorphous arrays composed of the different-sized silica particles of 190, 260, and 300 nm and PDDA using 10 cycles of the LbL method prepared on a clear glass plate and placed on the parallel nicols and crossed nicols.